JOURNAL OF MATERIALS SCIENCE 12 (1977) 873–883

A structural study of some SnO_2-Sb_2O_5 semiconducting glazes

R. H. TAYLOR
Central Electricity Research Laboratories, Kelvin Avenue, Leatherhead, Surrey, UK

The use of resistive glazes on high tension insulators to control flashover caused by pollution has proved only partially successful as a result of deterioration of the glazes in service. The most promising and now most widely used glaze relies upon the semiconducting properties of SnO_2 doped with Sb_2O_5, incorporated in an alumino-silicate base glaze. The structure of glazes containing various amounts of SnO_2 has been studied by a variety of techniques and particularly by scanning microscopy and electron probe microanalysis. These techniques have revealed both the existence and composition of relatively conducting and relatively insulating areas in the glaze, and a detailed analysis of the distribution of all the elements across the glaze surface and through the glaze thickness has been carried out. The results of this structural survey suggest that activated conduction proceeds through overlapping solubility rims around SnO_2 particles in the glaze.

1. Introduction

The idea of using a semiconducting glaze to control the surface resistivity, and hence the voltage distribution, on outdoor insulators was first proposed by Forrest [1] almost forty years ago. The clear advantages of such an idea (see, for example, Lambeth [2]) are largely offset, however by the progressive appearance of damage to the glazes in service. This is probably due to both electrolytic action and micro-discharging, and appears after only a few months in the worst cases. A number of different types of glazes have been developed, including ferrite glazes [3], partially reduced titania [4] and tin oxide doped with pentavalent antimony [5]. This last glaze has most nearly reached the standard of serviceability required for use in heavily polluted conditions and it is on this glaze that we focus our attention in the present paper.

Despite the use of doped tin oxide glazes in the production of high value resistors for high voltage applications [6], there exists little published material on their detailed structure or on the mechanism by which electrical conduction proceeds. A knowledge of these factors is believed to be fundamental to a deeper understanding of the more specific problem of the degradation of the glaze in service. In this paper, results are presented of a study of the structure of a number of types of tin oxide glaze, using the techniques of scanning electron microscopy and electron probe microanalysis (EPMA).

2. Experimental

The semiconducting glaze samples studied in this investigation were either home-made or provided by various manufacturers. The structures and electrical properties of the glazes were found to be relatively insensitive to the details of glaze preparation, firing times and temperatures. The home-made glazes were produced by calcining* Analar SnO_2 with 2.5 mol % Sb_2O_5 at 1200°C for a few hours and mixing the resulting powder into a base glaze of approximate composition SiO_2 70%, Al_2O_3 9%, $(NaK)_2O$ 4.5%, CaO 9% and ZnO 7.5%. The slurry was sprayed onto

*Samples in which the SnO_2 and Sb_2O_5 were not calcined but added separately to the base glaze somewhat surprisingly show similar structural and electrical character to the calcined glazes. Calcined glazes, however, do appear to give a lower temperature coefficient of resistance.

unfired electrical porcelain tiles which were then fired in air at 1200°C for 2 to 3 h. The samples were furnace cooled over a period of ~12 h. The fired glaze coated the porcelain to a thickness ~100 to 150 μm and for 15% SnO_2 samples, surface resistivities ~10^7 Ω/square were obtained.

The samples for analysis were in the form of short cylinders trepanned from the tiles using a diamond cutting tool. The bulk of the microscopy was performed on samples coated with a thin layer (~30 nm) of carbon or gold, to overcome the effects of charging in the electron beam of the scanning microscope. Elemental analysis was performed on a Cameca "Camebax" microprobe, the energy of the primary beam being selected to give a compromise between the requirements of spatial resolution and X-ray production efficiency. A beam voltage of ~15 kV was selected except where otherwise stated. Analysis has been carried out using three crystals; PET (penta-erythrytal tetranitrate, $a = 0.4375$ nm) LiF ($a = 0.201\,34$ nm) and for light element analysis ($Z \leqslant 14$) TAP (thallium acid phthallate, $a = 2.59$ nm).

3. General features of the glazes

Fig. 1 is a low magnification secondary electron scanning microscope picture and this shows a number of features typical of the glazes studied.

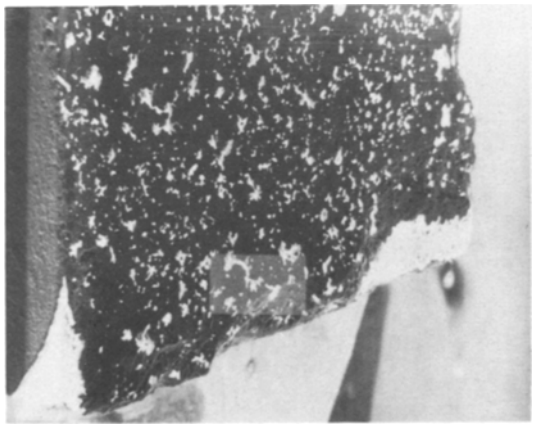

Figure 1 General view of an area of SnO_2–Sb_2O_5 glaze surface; × 30, 25 kV.

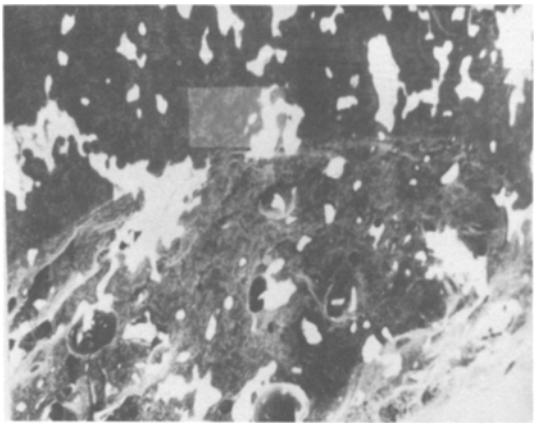

Figure 2 Higher magnification view of the high-lighted area from Fig. 1; × 210, 25 kV.

The most notable are the pronounced irregularly shaped white areas on the surface which are attributable to the effects of specimen-charging in the electron beam. One edge of this tile has been fractured, and examination of this fracture surface shows that the areas of charging also occur within the glaze thickness. Fig. 1 also reveals that there are many bubbles within the glaze, though fewer at the surface.

Fig. 2 shows a higher magnification study of the highlighted area in Fig. 1. Structure can now be seen in the dark areas between the charging regions; the mottled appearance at very high magnification being almost resolved into a network of submicron-sized particles which appear generally rounded. X-ray diffraction shows the predominant crystalline phase in the glaze to be SnO_2 and we identify the particles with this oxide.

When the charging of the surface is overcome by coating the exposed surface of the glaze with a thin layer of Au or C in an evaporator the appearance of the glaze is as shown in Fig. 3. It is difficult to correlate exactly the features of coated and uncoated samples since variation in the sample tilt and beam current may appreciably alter the precise shape and extent of the charging areas. Nonetheless, attempts have been made to compare a sample surface before and after depositing a Au film. The mottled areas remain visible in the coated sample and it becomes apparent that the areas which charge generally lie within relatively unmottled regions. It thus seems reasonable to assume that these latter areas are of lower conductivity than the rest of the glaze surface.

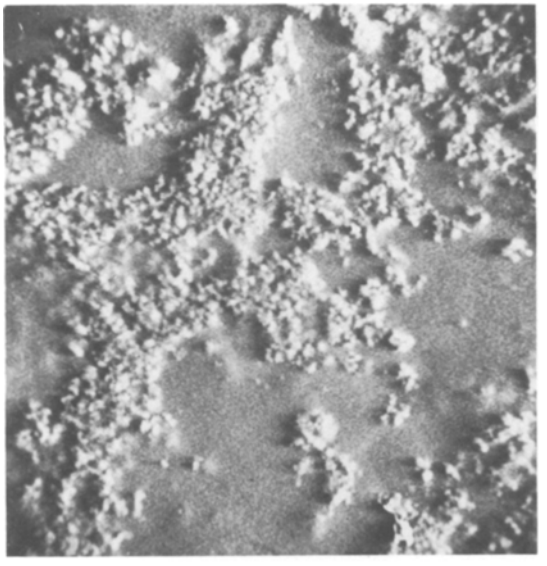

Figure 3 Scanning micrograph of a Au coated sample of glaze; × 4000, 30 kV.

Figure 4 View of an area on the glaze surface showing a high incidence of needle-shaped crystalline material; × 2000, 30 kV.

For samples with concentrations of less than about 20 to 25 mol % SnO_2, stereoscopic pairs of photographs taken on the scanning microscope show fairly gentle undulations of the surface. The charging areas appear to lie in the valleys. The form and spatial extent of the charging areas appears to be determined by the conditions for equilibrium between the flux of incident electrons and the rate at which charge is able to leak away through the glaze. This is vividly demonstrated by focusing a spot of electrons on a section of the dark background close to a charging area. Frequently, on re-rastering the electron spot, a micrograph may be obtained showing a freshly charged area around the position of the formerly stationary spot. The accumulation of charge then leaks away with a time constant of a few seconds. The degree of charging on "standard" glaze samples containing 15 to 20% SnO_2 was compared with the charging in samples containing up to 40% SnO_2. The same general features were observed at these higher concentrations but the extent of surface charging was reduced by a factor of about four. In samples containing more than 30% SnO_2, surface cracks were normally apparent.

High magnification, high resolution micrographs of the glaze surface reveal a further feature. High aspect ratio crystals (see Fig. 4) have been found in clusters in the glaze and an EPMA analysis of these crystals is described below. Estimates suggest that the crystals constitute considerably less than 5% of the glaze volume and lines from the crystals have not been observed in routine X-ray diffraction.

Hot-stage scanning micrographs are shown in Fig. 5. It is observed that as the temperature is taken above room temperature the charging areas on the glaze begin to fade. At a temperature ~200°C, there is hardly any evidence of surface charging and the high temperature micrograph again illustrates the fact that few SnO_2 crystallites exist in the areas which were charging at room temperature. It is clear from these results that the effect of raising the temperature is only to reduce the contrast due to charging and *not* to shrink the extent of such areas.

4. Electron microprobe analysis

4.1. Analysis of the glaze surface

Fig. 6(a) shows an elemental analysis in the energy range 2.6 to 4.1 keV obtained by focusing the primary electron beam on a mottled area of a glaze containing 30% SnO_2. The major contribution to the intensity comes from Sn and suggests that there is little contribution from K and Ca. Fig. 6(b) shows a similar elemental trace obtained by focusing the beam on an area of "background" glaze free from SnO_2 particles. In this case there is little contribution to the X-ray intensity from Sn and the strongest line in this energy range is the

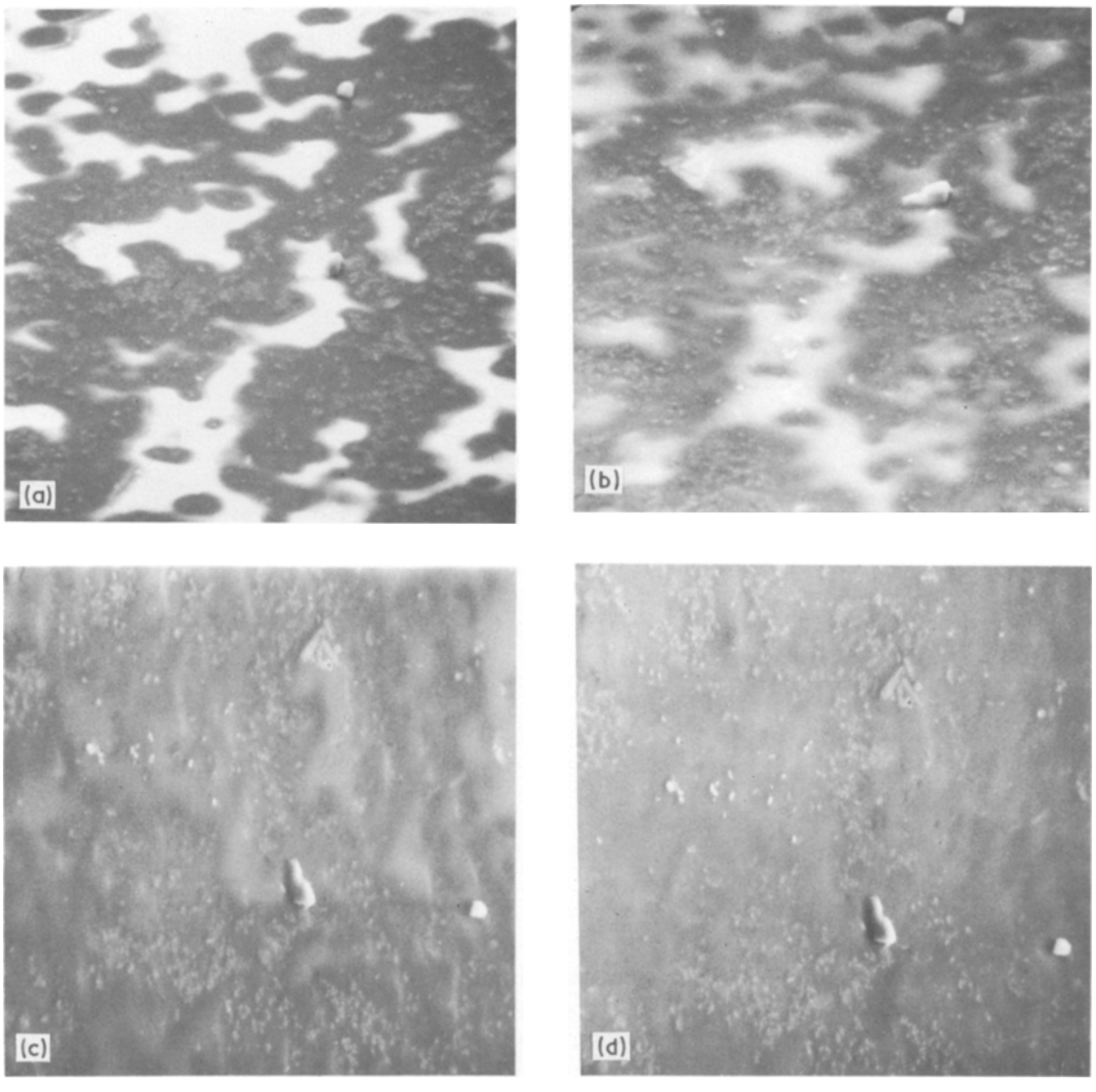

Figure 5 Scanning microscope pictures of an area of 15% SnO_2 glaze surface at (a) room temperature, (b) 100° C, (c) 150° C, (d) 200° C; × 700, 20 kV.

Ca$K\alpha$. In Fig. 6a eight lines can be clearly identified and higher resolution work enables a further Ca line ($K\beta_1$) to be identified as well as the Sb$L\alpha_1$ and $L\beta_1$ lines. The most intense of these two Sb lines, at maximum gain, gives a signal-to-noise ratio of ~10, and careful analysis of the peak-height ratios of the Sb lines to the Sn$L\alpha_1$ line gives a value of 3% for the concentration of Sb in the SnO_2 crystallites. This compares with the quoted value of 2.5 mol % and with the results of chemical analysis on a 15% SnO_2 glaze sample which gave a concentration of 2.8%. The results of this analysis strongly suggests that in the glaze, the Sb remains associated with the Sn and is not extensively dissolved in the surrounding glass.

Fig. 7 shows the covariation of the elements Sn, Sb, Ca, Al, Na, K and Si across a representative part of the surface of a 15% SnO_2 glaze. The results are typical of those obtained for all insulator glazes irrespective of SnO_2 concentration and the details of firing. The traces reveal that, in general, the elements Al, Na, K and Si contained in the original glass, give the same variation of X-ray intensity as a function of position. The Sn intensity is generally found to anticorrelate with the above elements, but the Ca intensity shows rather

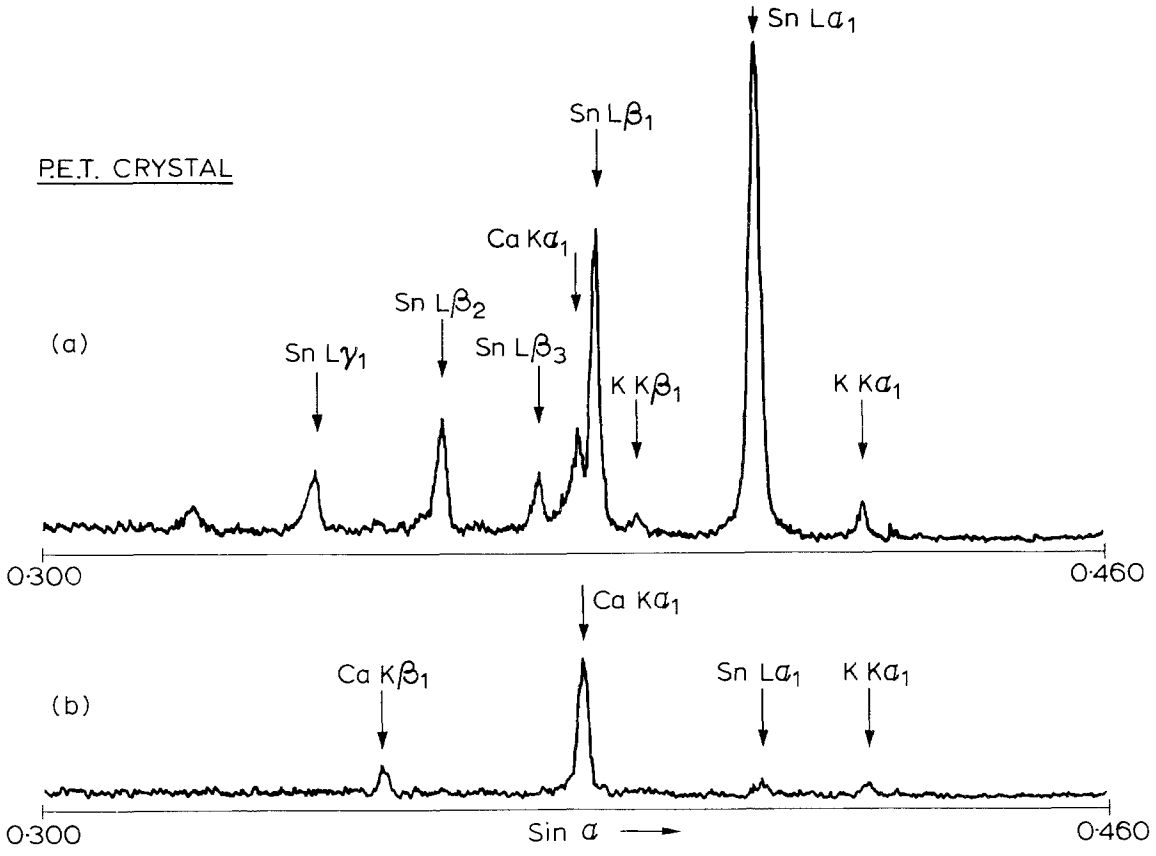

Figure 6 Electron probe analysis of (a) a high Sn area, (b) an area of background glaze from a 25% SnO_2 glaze. (10 kV) (PET crystal).

less consistent behaviour. Apart from a strong peak at point A, where the Sn X-ray intensity also peaks strongly, it shows little variation across the sample surface. The covariation of these two elements has been studied in some detail and comparison has been made with surface features in the scanning microscope. The points such as A, have been shown to be associated with the needle-shaped crystallites reported in Section 3. A point analysis from such a crystallite is shown in Fig. 8. This reveals that the major constituents of the crystals are Ca and Sn. These crystals appear throughout the volume of the glaze but it is difficult to estimate their distribution. Examination of the hot-stage pictures (Fig. 5) shows that these crystals lie in areas which charge in the scanning microscope.

In this investigation, another type of feature has occasionally been identified. At a number of points, a high Al X-ray count rate was obtained. These areas of high Al (approx. fifteen times as much Al relative to Si as in the usual base glaze) appear to correspond to raised strips on the surface which charge in the microscope beam. They appear amorphous and presumably result from phase separation in the glass.

A study of the width of the Sn peaks in the spectrometer as a function of position would, in principle, allow an estimate to be made of the extent of any Sn diffusion into the surrounding glaze. The solubility of Sn^{4+} into glasses has been shown to be low [7], and is unlikely to exceed $\sim 5\%$; however, as will be discussed in Section 5, the role of the Sn dissolved in the glaze is believed to be crucial to an understanding of the conduction mechanism in the bulk material. The form of the Sn distribution in Fig. 7 is typical of all the insulator glazes studied. Some of the peaks (such as B) appear to result from isolated SnO_2 particles, whilst the majority form part of a cluster. Careful studies of the isolated Sn peaks suggest that the intensity falls to zero over a distance of ~ 2 to $3\,\mu m$ from the centre of the Sn line. These results, however, must be treated

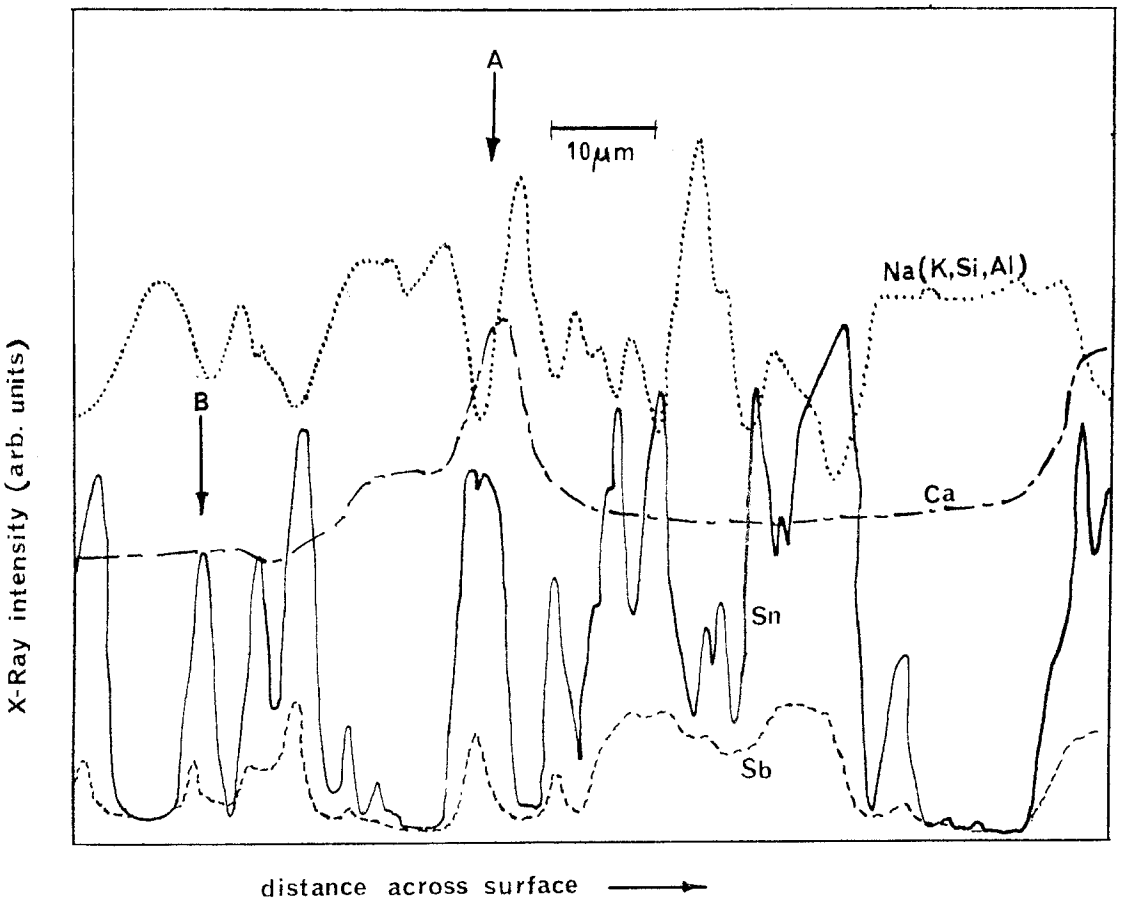

Figure 7 Covariation of the elements Sn, Sb, Ca and Na across a representative part of the surface of a 15% SnO_2 sample. The elements K, Si and Al show a similar variation to that shown by Na.

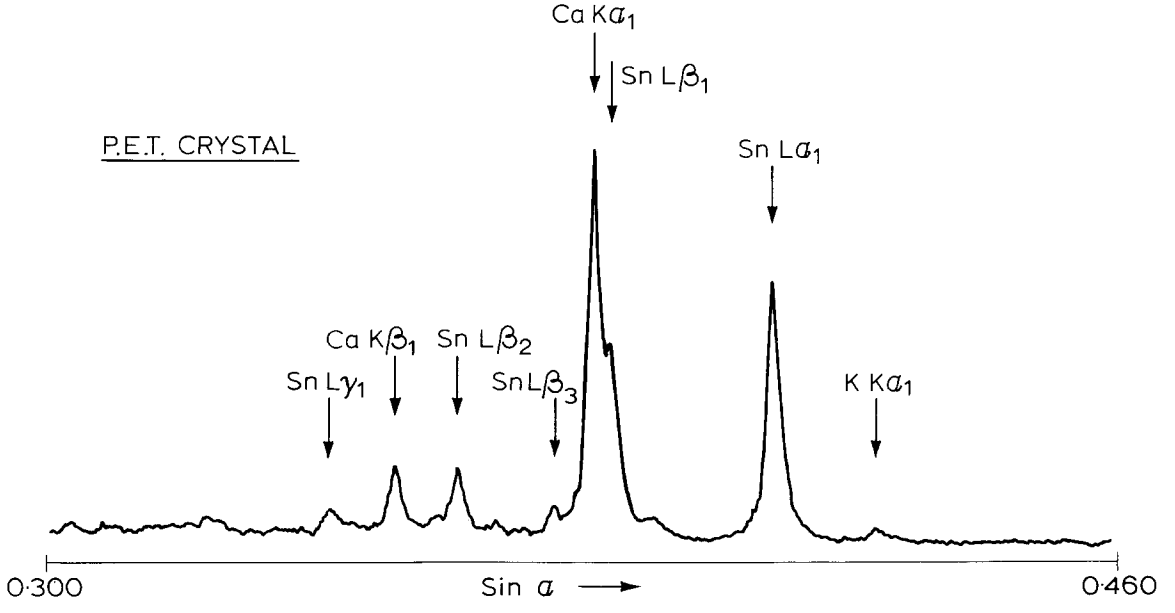

Figure 8 Electron probe microanalysis of a high aspect ratio crystalline area on the surface of a 30% SnO_2 glaze at 10 kV (PET crystal).

with caution. At 15 kV, the penetration of the primary beam in Si is ~2 μm [8] and there may be significant fluorescent radiation emerging from the volume surrounding the absorption volume of the beam. On a complex material containing submicron-sized particles it is clear that such effects may be important. An analysis of the solubility of SnO_2 single crystals in various base glaze systems is in progress.

The results of ESCA measurements on the glazes suggest that in the top few nanometres of an as-fired glaze surface, there are few SnO_2 crystallites. This result is confirmed by comparing the average X-ray intensity from areas on the surface of as-fired samples with areas from the surface of samples where the top few microns of glaze have been polished away. The X-ray intensity levels for the elements Si, Al, Na, Zn, Ca and K remain in much the same ratios between the two samples but the results show that, on average, in the top 2 μm or so of the glaze the average Sn intensity is some four times less than in the as-fired material.

The distribution of Sn close to the surface has been further analysed by reducing the primary beam voltage from 45 kV to 7.5 kV for the two types of samples. The penetration of the beam in a given element decreases linearly with the beam voltage [9]. Comparison of the intensities of the Ca$K\alpha$, Sn$L\alpha$, and K$K\alpha$, lines on a polished sample shows that the ratio of intensities remains constant to within 10% of its 45 kV value over the entire range of voltage. The form of the Sn:Ca and K:Ca ratio for the as-fired glaze as a function of accelerating voltage is shown in Fig. 9. For this sample (15% SnO_2) the K:Ca ratio remains constant to

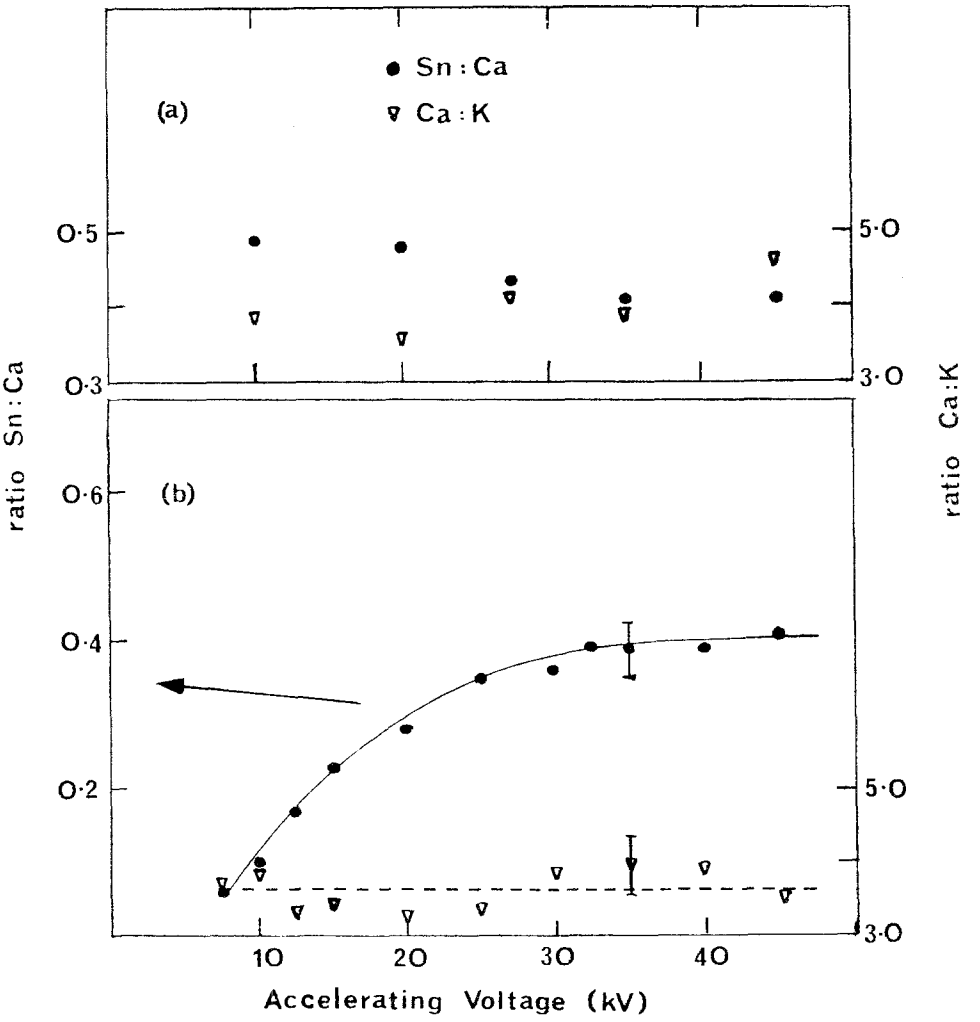

Figure 9 Ratio of Sn:Ca and Ca:K for (a) a ground sample surface, and (b) an unground as-fired sample surface (15% SnO_2).

within 10% over the entire voltage range, but below ~22 kV there is a steep decrease in the Sn:Ca ratio. This would imply that above 20 kV (penetration ~2.5 μm) the Sn-deficient surface represents a small proportion of the total probed volume. As the voltage is decreased, however, the volume deficient in Sn plays an increasingly significant role in determining the ratio. The fact that it is still rising at 10 kV, implies that either the Sn-deficient layer is less than 1 μm thick, or the layer is not in the form of a uniform "skin" of Sn-free glass, but rather in the form of a progressive Sn deficiency towards the surface. The second alternative seems the more likely. If SnO_2 crystallites are largely excluded from the top micron or so of the surface due to settling of the particles or surface tension effects, the form of the Sn:Ca ratio may provide some evidence for diffusion of Sn into the surrounding glaze. It may be appropriate to consider the deficient layer as the surface equivalent of the dissolution rim which we postulate to exist (see below, Section 5) around each SnO_2 particle. Removal of the surface does not significantly increase the bulk conductivity of the glaze, although if the surface was in the form of a skin of pure glass, its dielectric strength would be exceeded by an applied voltage in excess of a few volts.

A quantitative analysis of the results obtained here, however, is complicated by two further effects. Firstly the electron interaction of a solid is dependent upon both the beam voltage and the atomic number of the absorbing medium. Various theoretical relationships have been used with varying degrees of success to describe results for solids in ranges of energy between 5 keV and 30 keV [10]. A model of the glaze surface which postulates a "skin" of relatively light elements (essentially Ca and Si) containing a gradient of heavier material (Sn) implies a similar gradient in the electron-stopping efficiency of the material. In the present case, this will result in an underestimate of the real decrease of the Sn: Ca ratio as a function of reducing accelerating voltage. In addition the X-ray production efficiency in the material will depend upon the distribution of single and multiple scattering processes over the range of the electron. There is a marked increase in multiple scattering as the energy of the incident electron is attenuated by the solid. None of these remarks cast doubt upon the conclusion that the concentration of Sn is depth-dependent for the top few microns of glaze surface; the clearest evidence for this is contained in the comparison of results on ground and unground surfaces. The discussion does, however, point to the difficulties in obtaining quantiative information about the distribution of Sn.

This surface Sn depletion has been observed in a number of manufactured insulator glazes, its precise form showing variation from one type of sample to another.

4.2. Analysis of sections through the glazes

Polished sections were cut through two semiconducting glaze samples, one in which the SnO_2 and Sb_2O_5 had been calcined and one in which they had been added to the glaze separately. Fig. 10 shows in schematic form the variation of intensity from each element through the glaze thickness. The results for both samples were similar and good agreement was obtained from point to point on a given sample for most of the elements. In the scanning microscope, the porcelain–glaze boundary remains surprisingly sharp.

The distribution of Sn through the bulk of the sections was similar to the surface distribution and the Sb again correlated with the Sn. There was a tendency for strong Sn peaks to occur in clusters close to the glaze–porcelain interface and in a region about 10 μm below the upper surface. The Ca distribution was similar for all the samples studied. In each case the average Ca level peaked in a region between the centre of the glaze and a point about one quarter of the way in from the top surface. There was evidence for diffusion of Ca from the glaze into the porcelain to a distance of about 20 μm. Since Ca is known to behave as a blocking ion for the ionic transport of Na^+ and K^+, this diffusion into the porcelain may, therefore, have an important influence on the conductivity of the glaze. The silicon X-ray intensity showed a maximum near to the centre of the thickness, whilst the elements K and Al showed a maximum concentration of the glaze–porcelain interface with a reduction towards the surface. This seems to indicate diffusion from the porcelain into the glaze. In some samples, the Na concentration showed similar behaviour but in others a uniform distribution was observed. The behaviour of the Zn was again slightly variable. In general this distribution was fairly uniform, but again

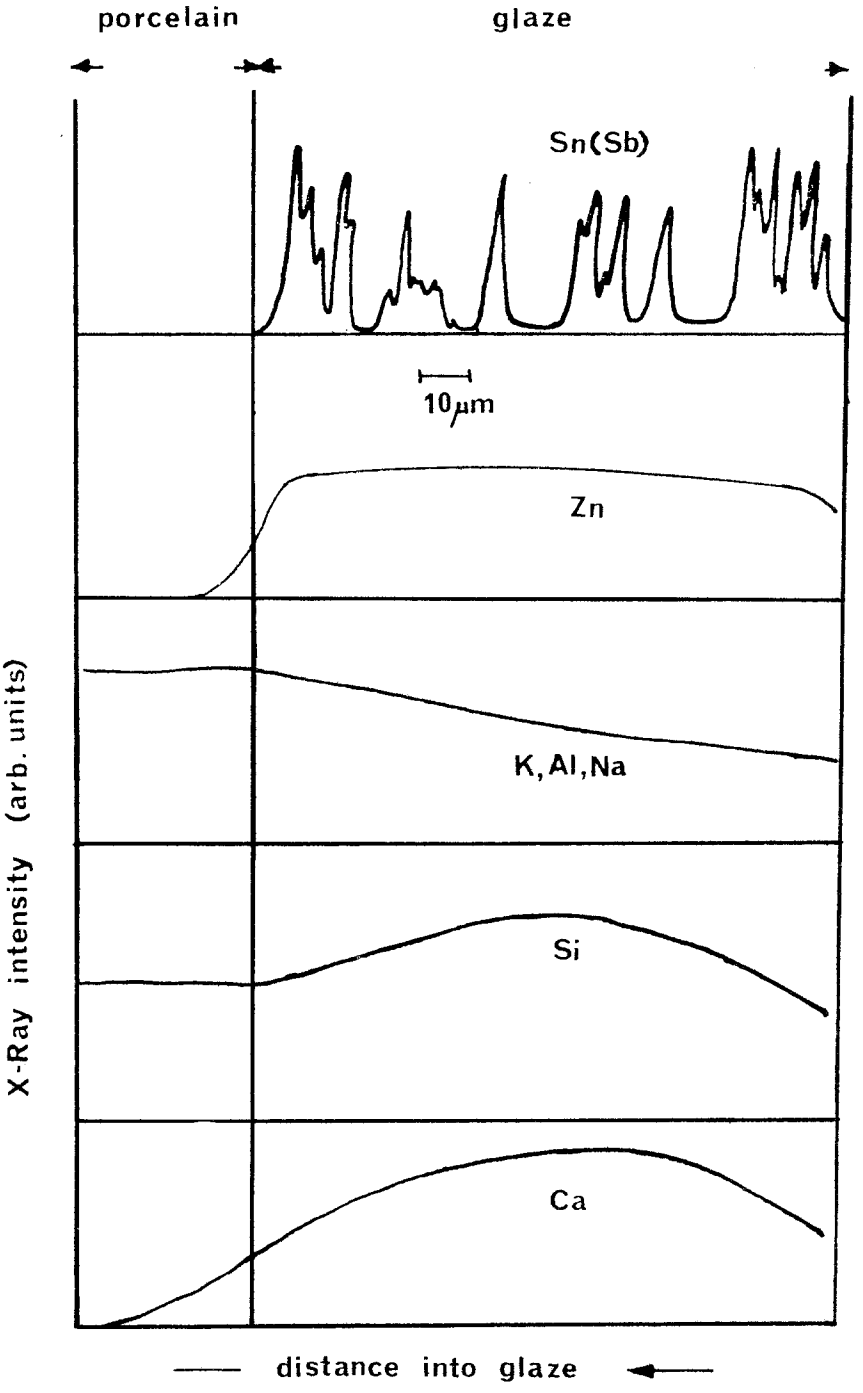

Figure 10 Schematic representation of the variation of X-ray intensities of the elements in the glaze across the glaze thickness.

there was a tendency for the intensity to decrease close to the top surface and some evidence for diffusion into the porcelain.

5. Conductivity in the materials

Results of detailed measurements of the conductivity of typical semiconducting glazes will not be presented in this paper, but the above analysis of the glaze structure clearly has implications for the electrical properties of these materials.

Pure SnO_2 is a dielectric with a band gap of 3.4 eV which may be substitutionally doped with Sb^{5+} to produce levels 0.03 eV below the conduction band. Single crystals of SnO_2 give typical

conductivities of $10^4 \Omega^{-1} m^{-1}$ [11], and pressed blocks of the SnO_2–Sb_2O_5 powder used in the glazes give a conductivity $\sim 1 \Omega^{-1} m^{-1}$ at 300 K. On the other hand, measurements of the conductivity of the base glaze used in these materials gives values $< 10^{-8} \Omega^{-1} m^{-1}$ at room temperature.

Samples of the glaze doped with SnO_2–Sb_2O_5 and fired under identical conditions give conductivities ranging from $\sim 10^{-7} \Omega^{-1} m^{-1}$ for a 10% addition of SnO_2 to a value $\sim 5 \times 10^{-4}$ $M^{-1} m^{-1}$ at 35% and the variation of log conductivity with volume fraction is linear. In systems where high conductivity is achieved by the establishment of a percolation path of interparticle contacts through the material, the transition from the non-conducting to the conducting state is normally sharp [12, 13].

This is clearly not the case in the insulator glazes and supporting evidence for the absence of a SnO_2–Sb_2O_5 conducting network in the material also comes from the non-linearity of V–I plots and from the fact that the glazes give a relatively high negative ($\sim 1\%$ deg^{-1}) temperature coefficient of resistance. Transmission electron micrographs also lend support to the view that the individual SnO_2 crystallites do not touch [17]. These results are in contrast with the electrical properties of the Sb-doped SnO_2 glazes used in the production of high value high stability resistors [6]. In this case the glazes are produced by sintering ultrafine oxide powders with ground glass and are rapidly cooled. The resulting glazes have temperature coefficients as low as $10^{-1}\%$ deg^{-1} and display highly linear V–I characteristics. We have not studied the concentration dependence of the conductivity in these materials but it seems likely that conduction is achieved largely by direct interparticle contact.

The smooth variation of conductivity, as the proportion of conducting phase is increased in the insulator glazes, might be better explained by postulating the existence of overlapping "solubility rims" between the crystallites of SnO_2 [14, 15]. The absence of a sharp cut-off in the extent of these rims will lead to an extended transition regime for the conductivity as a function of concentration. Some experimental evidence for the existence of these areas comes from the SEM pictures where the non-charging regions may be pictured as providing a percolation path of relatively conducting material. The hot-stage results demonstrate that at temperatures above about 450 K, the ionic conductivity of the undoped glass has increased enough to avoid specimen charging and the whole glaze has become relatively conducting. The form of plots of conductivity against reciprocal temperature for the glazes, indicate that whilst the electronic component of the conductivity is dominant below about 500 K, above these temperatures the ionic conductivity of the undoped glaze predominates. At room temperature, for a typical 15% SnO_2 glaze the transport number is $\sim 10^{-4}$. Although the ionic term contributes little to the total conductivity, over the many thousands of hours during which a typical glaze is excited, electrolytic damage may still be important.

This analysis avoids the question of how electrical conduction is achieved in the rims. Doped amorphous materials are usually not semiconductors since the structure adjusts itself so that any atom has the right number of neighbours to accommodate all the electrons in bonds. Since both the Sn and Sb solubilities in the glaze are low, it is difficult to envisage a situation in which close association of Sn and Sb atoms could occur in the rims. It is possible that activated conduction may be achieved in these regions between the particles as a result of local effects akin to the results of off-stoichiometry in pure SnO_2 [15]. In bulk SnO_2, off-stoichiometry produces levels 0.3 eV into the gap [16].

6. Conclusions

A fairly detailed picture of the structure of SnO_2–Sb_2O_5 semiconducting glazes has been obtained by a combination of scanning electron microscopy and electron microprobe analysis. It has revealed:

(1) The existence and composition of relatively conducting and relatively insulating areas in the glaze and the effects of varying the proportion of the conducting material in the glaze and the temperature.

(2) The distribution and morphology of the Sn and the association of the Sn and Sb in the SnO_2 crystallites.

(3) The existence of small amounts of a crystalline phase rich in Sn and Ca in the form of needle- and diamond-shaped crystals. Some evidence has been presented for the separation of an Al-rich phase in the glass.

(4) The existence (and possible form) of a Sn depleted layer at the as-fired surface of the glaze.

(5) The distribution of elements through the glaze thickness. In particular, the existence of Ca diffusion into the base porcelain.

(6) That the electrical conductivity in the materials probably arises from the overlap of Sn solubility rims around the SnO_2 crystallites. Conductivity is thought to arise from local effects on the network similar to those produced by off-stoichiometry at a particular site, leading to activated conduction.

Acknowledgements

I would particularly like to thank Mr P.W. Teare for extremely valuable discussions on many aspects of the experimental techniques. I would also like to thank Dr J. Robertson and Mr B.J. Maddock of CERL and Dr D. Allinson of NPL for useful comments, and Dr G. Hill of the Electrical Research Association for obtaining the high temperature scanning microscopy pictures. The work was carried out at the Central Electricity Research Laboratories and is published by permission of the Central Electricity Generating Board.

References

1. J. S. FORREST, *J. Inst. Elect. Eng.* **79** (1936) 401.
2. P. J. LAMBETH, *I.E.E. Rev.* **118** (1971) 1107.
3. J. S. FORREST, *J. Sci. Instrum.* **24** (1947) 211.
4. D. G. POWELL, *Bull. Amer. Ceram. Soc.* **52** (1973) 600.
5. D. B. BINNS, *Trans. Brit. Ceram. Soc.* **73** (1974) 7.
6. J. DEARDEN, "Electronic Components" March 1967.
7. J. S. SIEGER, *J. Non-Crystalline Solids,* **19** (1975) 213.
8. C. A. ANDERSEN, in "The Electron Microprobe" (John Wiley, New York, 1966) p. 50.
9. J. C. RUSS, in "Energy Dispersion X-Ray Analysis" (ASTM Special Technical Publication, 1971) p.154.
10. V. E. COSLETT and R. N. THOMAS, "The Electron Microprobe" (John Wiley, New York, 1966) p. 248.
11. J. A. MARLEY and R. C. DOCKERTY, *Phys. Rev.* **140** (1965) 304.
12. D. B. BINNS, *Trans. Brit. Ceram. Soc.* **73** (1974) 1.
13. B. ABELES, H. L. PINCH and J. I. GITTLEMAN, *Phys. Rev. Letters* **35** (1975) 247.
14. R. J. BROOK, D. GILLING, K. T. HARRISON, B. HUDSON, A. E. HUGHES, D. WRIGHT, D. TAYLOR and C. E. RICKETTS, Proceedings of the conference on Electrical and Optical Properties of Glasses and Ceramics, (Brit. Ceram. Soc., St. Andrews, April 1976) p. 4.
15. R. H. TAYLOR and J. ROBERTSON, *ibid* p. 3.
16. E. LEJA, *Acta Phys. Pol.* **A33** (1970) 165.
17. D. ALLINSON, T. BARRY and R. M. TAYLOR, (to be published).

Received 9 September and accepted 21 October 1976.